Electronic Supplementary Material (ESI) for ChemComm.

Supporting Information

Tuning the Pore Chemistry of Zr-MOFs for Efficient Metal Ion Capture from Complex Streams

R. Eric Sikma,[a] Boyoung Song,[b] Jacob I. Deneff,[a] Jacob Smith,[b] Kadie Sanchez,[b] Raphael A. Reyes,[a] Luke M. Lucero,[a] Keith J. Fritzsching,[c] Anastasia G. Ilgen,[b] Dorina F. Sava Gallis*[a]

[a]Nanoscale Sciences Department, Sandia National Laboratories, Albuquerque, NM 87185, United States

[b]Geochemistry Department, Sandia National Laboratories, Albuquerque, NM 87185, United States

[c]Organic Materials Science Department, Sandia National Laboratories, Albuquerque, NM 87185, United States

Materials and Methods.

General. All reagents and solvents were purchased from commercial suppliers and used without further purification. Powder X-ray diffraction measurements were performed on a Bruker D2Phaser instrument using CuKα radiation (λ = 1.54178 Å). Infrared spectra were collected on a Thermo Scientific Nicolet iS20 FTIR spectrometer with a Smart iTX diamond ATR. Samples for gas sorption were exchanged with methanol or acetone and activated at 120 °C (UiO-66 derivatives) or 150 °C (MOF-808 derivatives) under high vacuum for 12 h. N_2 adsorption isotherms were collected at 77 K on a Micromeritics ASAP 2020 surface area and porosity analyzer using ultra-high purity nitrogen (99.999%, obtained from Matheson Tri-Gas). The isotherms were analyzed using the Micromeritics Microactive software. Thermogravimetric analysis (TGA) was conducted on a TA SDTQ600 instrument. Activated MOF samples were heated to 900 °C at a ramp rate of 10 °C min^{-1} under continuous air flow.

Synthesis of UiO-66(HD). UiO-66(HD) was synthesized following a literature procedure.[1] Benzene-1,4-dicarboxylic acid (0.166 g, 1.00 mmol), $ZrCl_4$ (0.233 g, 1.00 mmol), and benzoic acid (2.44 g, 20.0 mmol) were added to a 100 mL screw-top jar with a PTFE-lined lid. N,N-dimethylformamide (DMF) (18 mL) was added and the solids were dissolved by sonication. The reaction was heated to 120 °C in an isothermal oven for 48 h. The resulting white solid was collected by centrifugation and washed with DMF (3 x 30 mL), then transferred to a clean 100 mL jar and suspended in 20 mL of fresh DMF. Hydrochloric acid (12.1 M, 0.40 mL) was added and the suspension was well-mixed, then heated to 90 °C in an isothermal oven for 12 h. The solid was then collected by centrifugation and washed with DMF (3 x 30 mL) and MeOH (3 x 30 mL) over 3 days. The white solid was dried and activated under vacuum at 120 °C for 12 h prior to use. All characterization data matched previous literature reports.

Synthesis of UiO-66(LD). UiO-66(LD) was synthesized following a literature procedure.[2] DMF (19.5 mL) was added to a 100 mL jar, followed by the addition of $ZrCl_4$ (0.756 g, 3.24 mmol). Concentrated hydrochloric acid (0.572 mL) was then added and the mixture was sonicated to fully dissolve the $ZrCl_4$. Benzene-1,4-dicarboxylic acid (1.08 g, 6.49 mmol) was then added to the solution and fully dissolved by sonication. The solution was equally distributed into 4 PTFE-lined steel autoclaves, which were then sealed and heated to 220 °C for 20 h. The resulting white solid was collected by centrifugation and washed with DMF (3 x 30 mL) and methanol (3 x 30 mL) over 3 days. The MOF was then activated at 120 °C for 20 h prior to use. All characterization data matched previous literature reports.

Synthesis of UiO-66-NH_2(HD). UiO-66-NH_2(HD) was synthesized following a literature procedure.[3] $ZrCl_4$ (1.26 g, 5.4 mmol) and concentrated hydrochloric acid (10.0 mL) were added to 50 mL of DMF and sonicated until complete dissolution of $ZrCl_4$. A solution of 2-aminoterephthalic acid (1.36 g, 7.5 mmol) in 100 mL DMF was then added to the metal solution and the solutions were well-mixed (total volume = 150 mL). The resulting solution was distributed evenly into six 100 mL jars with PTFE-lined lids (25 mL per jar), then heated to 60 °C in an isothermal oven for 18 h. The resulting light-yellow solid was collected by centrifugation and washed with DMF (3 x 50 mL) and acetone (3 x 50 mL) over 3 days. The MOF was then activated at 120 °C for 20 h prior to use. All characterization data matched previous literature reports.

Synthesis of UiO-66-NH_2(LD). UiO-66-NH_2(LD) was synthesized following a literature procedure.[3] $ZrCl_4$ (1.26 g, 5.4 mmol) and concentrated hydrochloric acid (1.00 mL) were added to 50 mL of DMF and sonicated until complete dissolution of $ZrCl_4$. A solution of 2-aminoterephthalic acid (1.36 g, 7.5 mmol) in

100 mL DMF was then added to the metal solution and the solutions were well-mixed (total volume = 150 mL). The resulting solution was distributed evenly into six 100 mL jars with PTFE-lined lids (25 mL per jar), then heated to 120 °C in an isothermal oven for 18 h. The resulting light-yellow solid was collected by centrifugation and washed with DMF (3 x 50 mL) and acetone (3 x 50 mL) over 3 days. The MOF was then activated at 120 °C for 20 h prior to use. All characterization data matched previous literature reports.

Synthesis of MOF-808. MOF-808 was synthesized following a modified literature procedure.[4] Trimesic acid (0.210 g, 1.00 mmol) and $ZrOCl_2 \cdot 8H_2O$ (0.970 g, 3.01 mmol) were added to a 250 mL screw-top jar with a PTFE-lined lid. The solids were dissolved in a mixture of 30 mL DMF and 30 mL formic acid, then the reaction was heated to 100 °C in an isothermal oven for 24 h. The resulting white solid was washed with DMF (3 x 30 mL) and acetone (3 x 30 mL) over a period of 3 days, then dried in a vacuum oven at 85 °C for 12 h prior to use. All characterization data matched previous literature reports.

Synthesis of UiO-66-NHPAA. Phosphonoacetic acid (0.072 g, 0.51 mmol) and dicyclohexylcarbodiimide (DCC, 0.141 g, 0.68 mmol) were added to a 250 mL round-bottom flask, followed by the addition of 80 mL acetonitrile. UiO-66-NH_2(LD) (0.100 g) was added to the flask, then the resulting suspension was heated with stirring to 85 °C for 24 h under a water-cooled condenser. The solid was then collected by centrifugation and washed with DMF (3 x 20 mL), methanol (3 x 20 mL), and dichloromethane (3 x 20 mL), with a minimum of one overnight soak per unique solvent. The solid was then dried at 85 °C under vacuum for 12 h to give UiO-66-NHPAA as a light-yellow solid. Successful incorporation of phosphonate groups was confirmed by IR spectroscopy and solid-state ^{13}C and ^{31}P NMR.

Synthesis of MOF-808-PyC. MOF-808 (0.200 g) and pyrazole-4-carboxylic acid (PyC, 0.537 g, 4.40 mmol) were added to a 100 mL screw-top jar. DMF (20 mL) was added and the resulting suspension was sonicated to fully dissolve PyC. The jar was sealed and the reaction was heated to 60 °C in an isothermal oven for 18 h. The solid was then collected by centrifugation and washed with DMF (3 x 30 mL) and acetone (3 x 30 mL), then dried at 85 °C under vacuum for 12 h to give MOF-808-PyC as a white solid. Incorporation of PyC was confirmed by IR spectroscopy and ^1H NMR of a digested sample.

Synthesis of MOF-808-Et_2PAA. Diethylphosphonoacetic acid (Et_2PAA, 0.431 g, 2.20 mmol) was weighed into a 20 mL vial in a N_2-filled glovebox and dissolved in 10 mL dry DMF. MOF-808 (0.200 g) was added to a 50 mL glass pressure vessel, followed by the addition of the Et_2PAA solution. The Et_2PAA solution was transferred quantitatively by rinsing the vial twice with 5 mL dry DMF and adding the rinses to the reaction vessel, giving a total volume of 20 mL for the reaction. The vessel was sealed under N_2 then heated to 100 °C in an isothermal oven for 18 h. The solid was then collected by centrifugation and washed with DMF (3 x 30 mL) and acetone (3 x 30 mL), then dried at 85 °C under vacuum for 12 h to give MOF-808-Et_2PAA as a white solid. Incorporation of Et_2PAA was confirmed by IR spectroscopy and ^1H NMR of a digested sample.

Synthesis of MOF-808-AA. MOF-808 (0.200 g) and aspartic acid (AA, 0.586 g, 4.40 mmol) were added to a 100 mL screw-top jar. Deionized H_2O (20 mL) was added and the resulting suspension was sonicated to fully dissolve AA. The jar was sealed and the reaction was heated to 60 °C in an isothermal oven for 18 h. The solid was then collected by centrifugation and washed with deionized H_2O (3 x 30 mL) and acetone (3 x 30 mL), then dried at 85 °C under vacuum for 12 h to give MOF-808-AA as a white solid. Incorporation of AA was confirmed by IR spectroscopy and ^1H NMR of a digested sample.

Synthesis of MOF-808-BDC-SO_3. The procedure was identical to the synthesis of MOF-808-AA using 5-sulfoisophthalic acid monosodium salt (BDC-SO_3, 1.18 g, 4.40 mmol) in place of AA. Incorporation of BDC-SO_3 was confirmed by IR spectroscopy and ^{1}H NMR of a digested sample.

Synthesis of MOF-808-AA/BDC-SO_3. The procedure was identical to the synthesis of MOF-808-AA using a combination of AA (0.293 g, 2.20 mmol) BDC-SO_3 (0.590 g, 2.20 mmol) in place of AA. Incorporation of AA and BDC-SO_3 was confirmed by IR spectroscopy and ^{1}H NMR of a digested sample.

Solid-State NMR. The samples were packed into 2.5 mm Bruker style MAS rotor. All experiments were performed on a 600 MHz Bruker Advance III instrument. The MAS rate was set to 33.333kHz. Cross polarization experiments were collected with a recycle delay (d_1) of 2 s or 4 s. The ^{31}P data was collected with a recycle delay of 5 s. The ^{13}C spectra were averaged over 20,480 to 30,720 scans, and the ^{31}P spectra was averaged over 1024 scans. The intensity of the ^{13}C spectrum was scaled by $1/(1 - exp(-d_1/T_{1,H}))$ where $T_{1,H}$ was measured in an ^{1}H inversion recovery experiment. Spectra were deconvoluted and plotted in python using the nmglue package.

The solid-state cross-polarization (CP) magic-angle-spinning (MAS) ^{13}C spectra of UiO-66-NH_2 and UiO-66-NHPAA are shown in main text figures 3B and 3C, respectively. Due to disorder the peaks are broad, nevertheless there is enough resolution to estimate the lower bound of the UiO-66-NHPAA conversion. The UiO-66-NH_2 peak at $\delta_C = 142.7\ ppm$ is assigned to the aromatic carbon bound to nitrogen. Likewise, The UiO-66-NHPAA peak at $\delta_C = 149.6\ ppm$ is assigned to the aromatic carbon bound to nitrogen. In the UiO-66-NHPAA spectrum, the $\delta_C = 142.7\ ppm$ peak is unresolved, but at maximum there is 60% of the intensity in the regions as in UiO-66-NH_2. The CP dynamics would be expected to be similar for these two peaks; therefore, we estimate the lower bound of conversion by comparing the integrals of the deconvoluted spectra. In the UiO-66-NHPAA spectrum I($149.6\ ppm$) / (I($149.6\ ppm$) + 0.6 $\times I\ (142.7\ ppm)$) = 63 %, were I(ppm) is the integral of the deconvoluted spectrum. We estimate that the error in this analysis is < 10 %. The NH_2 to NHPAA conversion is then > 63 $\pm$ 10 %. The UiO-66-NHPAA spectrum is consistent with a minor fraction of phosphonoacetic acid moieties that that were incorporated in a different manner.

The solid-state ^{31}P spectrum UiO-66-NHPAA is shown in Figure S4. Three peaks are observed. The most intense fraction near $\delta_P =$ 11.8 ppm is assigned to the amide-linked NHPAA groups. The smaller fractions likely result from phosphonoacetic acid that is bound to Zr metal clusters directly through either the carboxylate or the phosphonate groups.

MOF digestion and solution NMR. Approximately 30 mg of MOF was added to 20 mL vials, followed by the addition of KOD (75 µL, 30% in D_2O) and D_2O (0.75 mL). The resulting suspensions were stirred at room temperature for 18 h to fully dissolve the carboxylated organics, then the remaining solid ZrO_2 was removed using a 13 mm PTFE membrane syringe with a 0.2 µm pore size. ^{1}H NMR spectra of the resulting clear solutions were collected using a 500 MHz Bruker Advance II Spectrometer, and the data were analyzed using Bruker Topspin software. The integration of the 1,3,5-benzenetricarboxylate (BTC) singlet at ~8.32 ppm was set to 3 and the integrations of functional group peaks were used to determine the BTC/functional group ratios. The number of functional groups per Zr_6 cluster was determined by assuming 2 BTC molecules per cluster, as determined from the ratio in the crystal structure.

Competitive metal ion adsorption experiments. An aqueous solution containing approximately 0.2 mM of $Co(NO_3)_2$, $Ni(NO_3)_2$, $Nd(NO_3)_2$, and $Lu(NO_3)_2$ in 100 mM HEPES buffer (HEPES = 2-[4-(2-hydroxyethyl)piperazin-1-yl]ethanesulfonic acid) was prepared, and the initial concentration of each ion was determined by inductively coupled plasma-mass spectrometry (ICP-MS) using a NexION 350D instrument. The precise concentrations were determined in normal mode by reference to calibration curves (R^2 = 0.9999 or higher) obtained from certified standard solutions with known concentrations for each ion. Activated MOF powder (50 mg) was added to a 50 mL polypropylene centrifuge tube and submerged in 20 mL of the mixed-ion solution. The pH was recorded at the beginning and end of the experiment and was found to remain at 6.5 (± 0.2) throughout. The resulting suspension was agitated using a shaker for 24 h, then the suspension was filtered through a 0.2 µm Nylon syringe filter (Millex®). The solution was subsequently acidified by the addition of 0.3 mL of 6M HNO_3 (ultrahigh purity, and analyzed by ICP-MS to determine the final concentration of each ion. The adsorbed quantities of the ions were determined as the difference between the initial and final mmol quantities in solution, which were used to calculate removal percentages (i.e., removal efficiencies, main text Figure 5).

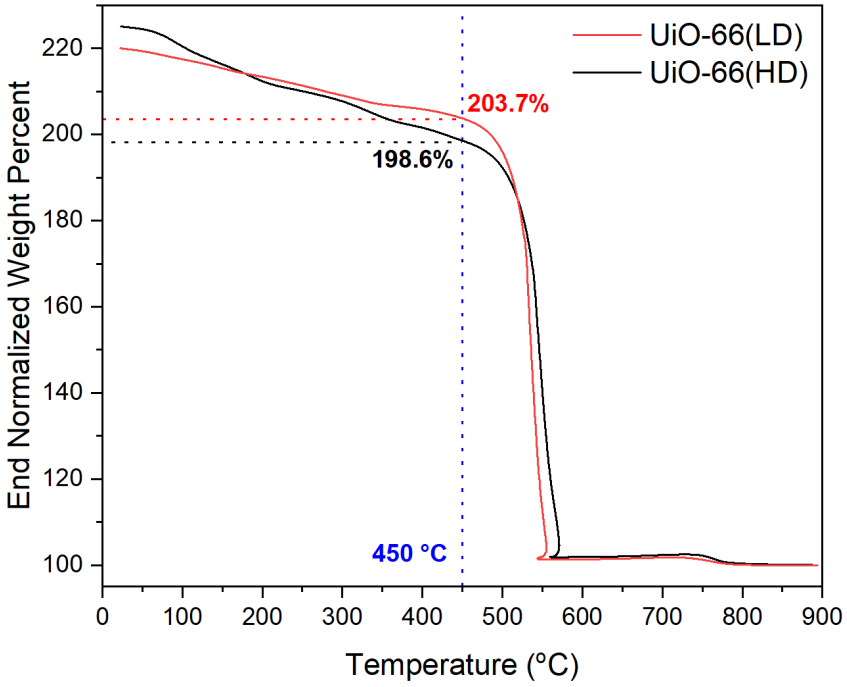

Figure S1. End-normalized TGA data for UiO-66(HD) (black trace) and UiO-66(LD) (red trace) collected under air; the higher wt.% of UiO-66(LD) at 450 °C is attributed to fewer missing linker defects.[2]

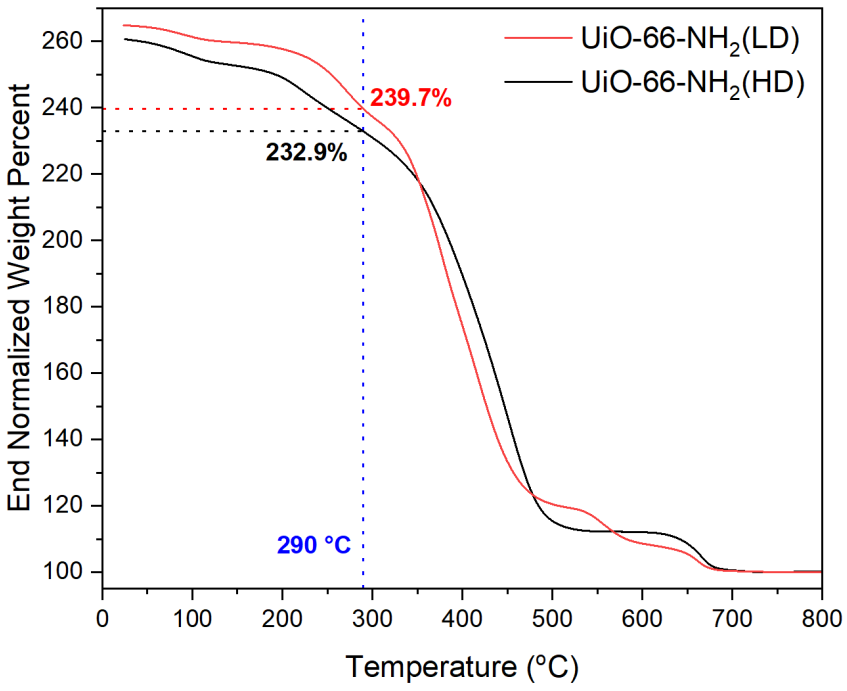

Figure S2. End-normalized TGA data for UiO-66-NH_2(HD) (black trace) and UiO-66-NH_2(LD) (red trace) collected under air; the higher wt.% of UiO-66-NH_2(LD) at 450 °C is attributed to fewer missing linker defects.[2]

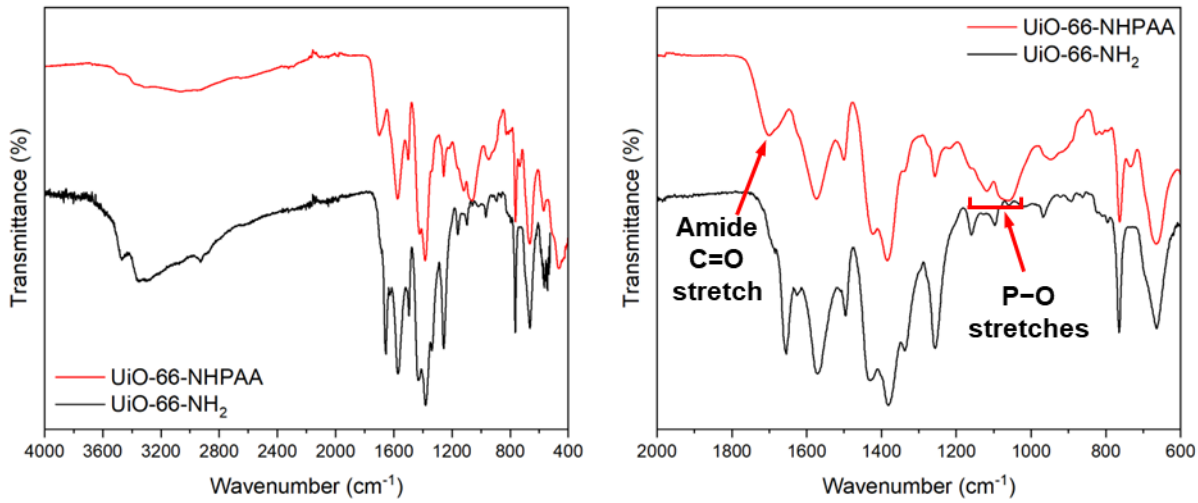

Figure S3. Full (left) and zoomed in (right) infrared spectra of UiO-66-NH_2 and UiO-66-NHPAA.

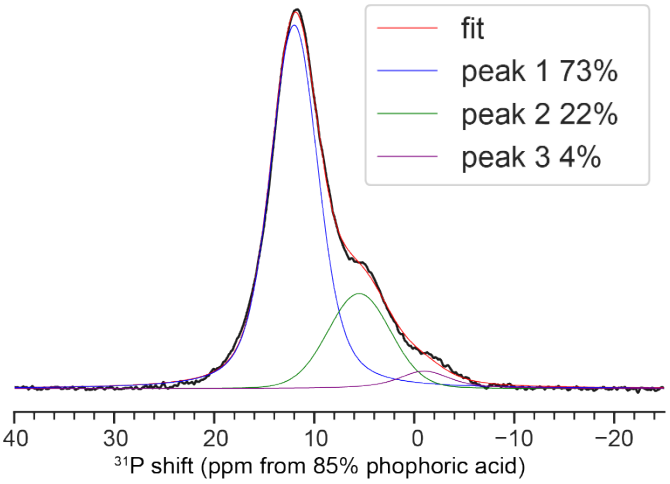

Fi

Figure S4. ^{31}P MAS NMR spectrum of UiO-66-NHPAA. Deconvoluted sub-spectra for three peaks and their sum are shown with colored lines.

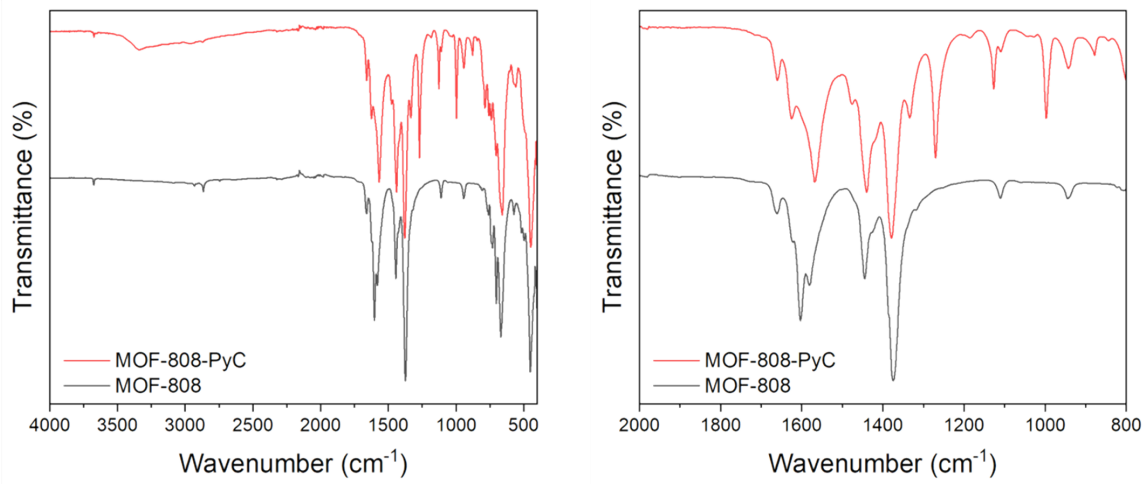

Figure S5. Full (left) and zoomed-in (right) IR spectra of MOF-808-PyC (red) and unmodified MOF-808 (black).

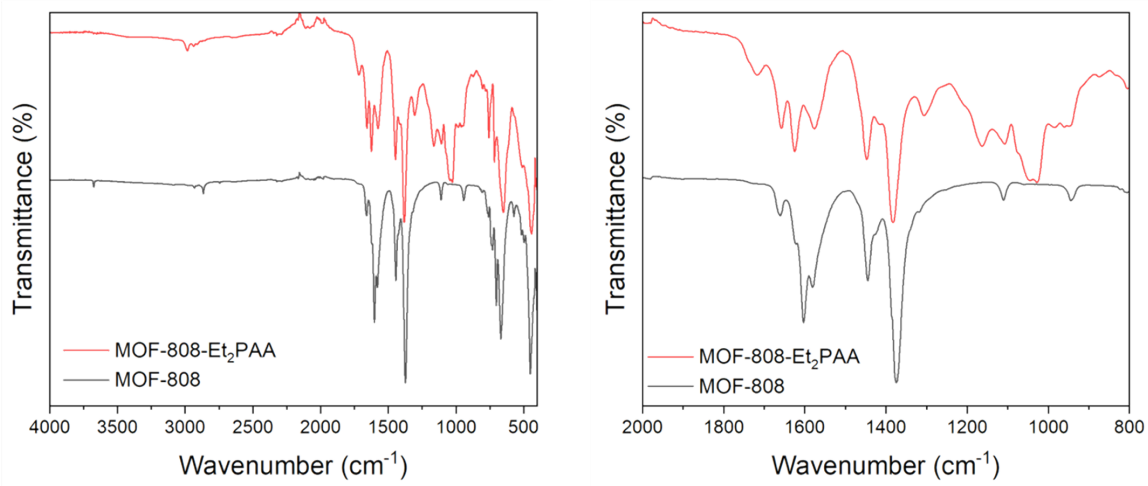

Figure S6. Full (left) and zoomed-in (right) IR spectra of MOF-808-Et_2PAA (red) and unmodified MOF-808 (black).

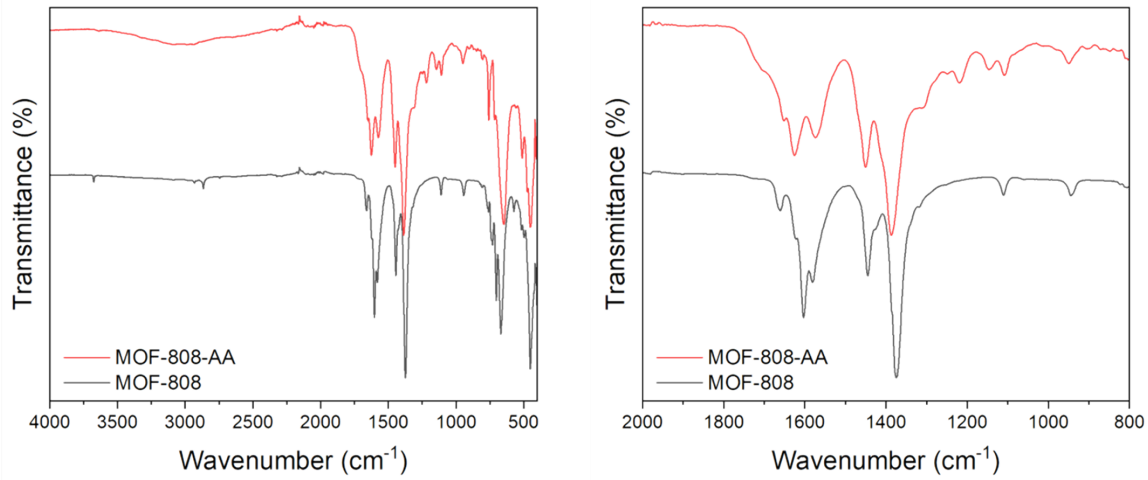

Figure S7. Full (left) and zoomed-in (right) IR spectra of MOF-808-AA (red) and unmodified MOF-808 (black).

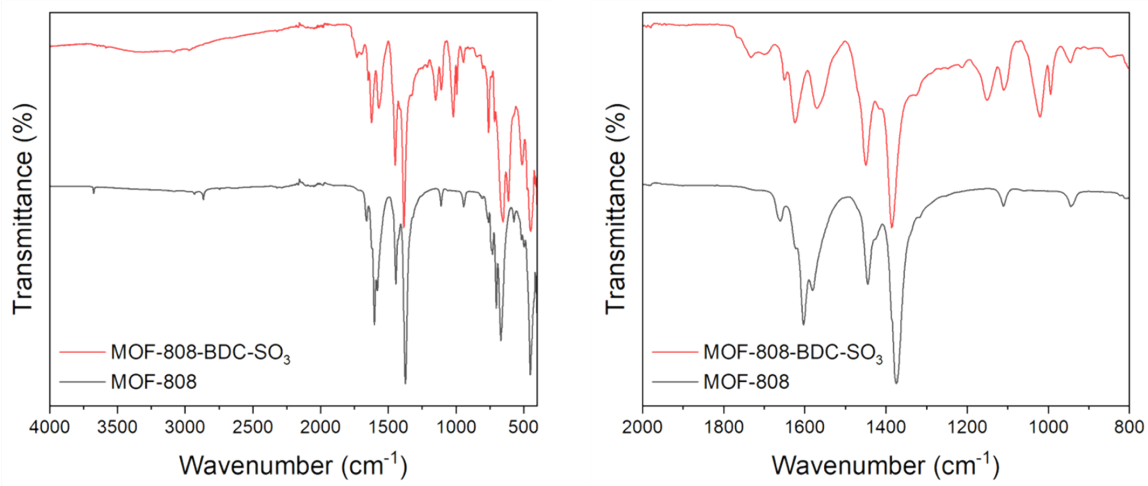

Figure S8. Full (left) and zoomed-in (right) IR spectra of MOF-808-BDC-SO_3 (red) and unmodified MOF-808 (black).

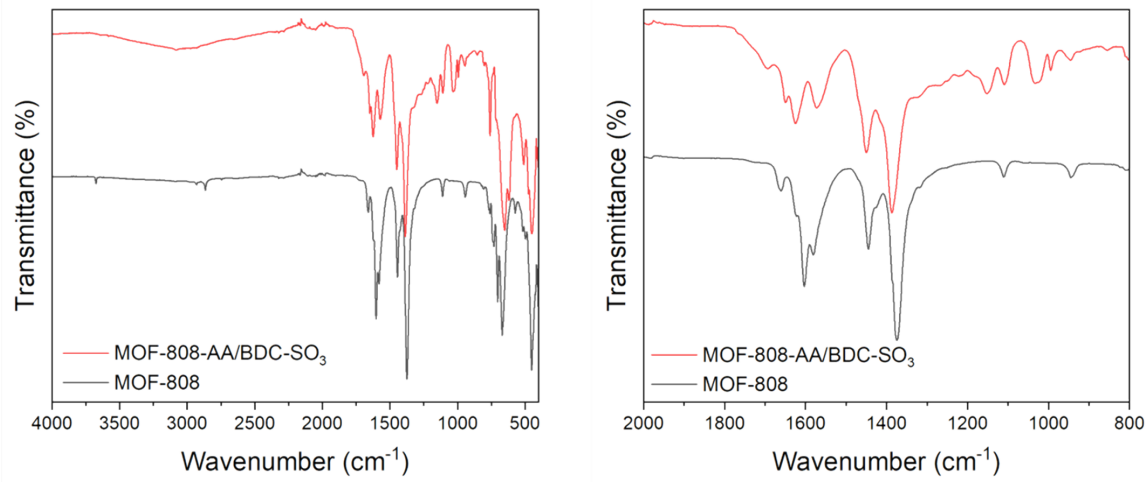

Figure S9. Full (left) and zoomed-in (right) IR spectra of MOF-808-AA/BDC-SO_3 (red) and unmodified MOF-808 (black).

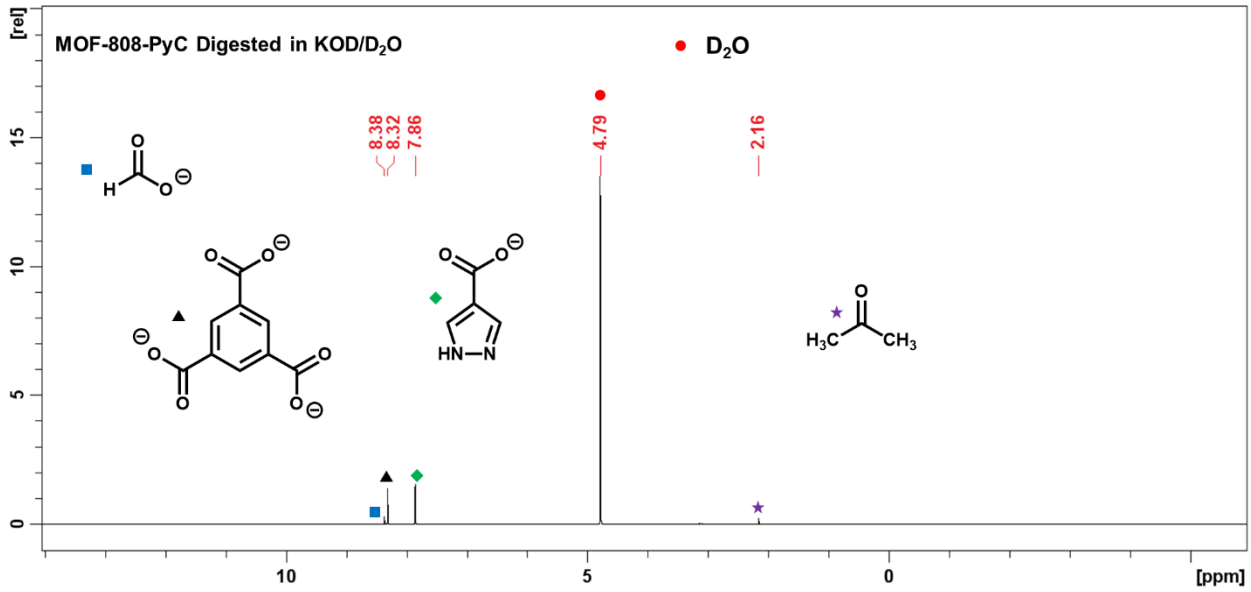

Figure S10. ^{1}H NMR spectrum of MOF-808-PyC digested in KOD/D_2O. A minor acetone impurity is present.

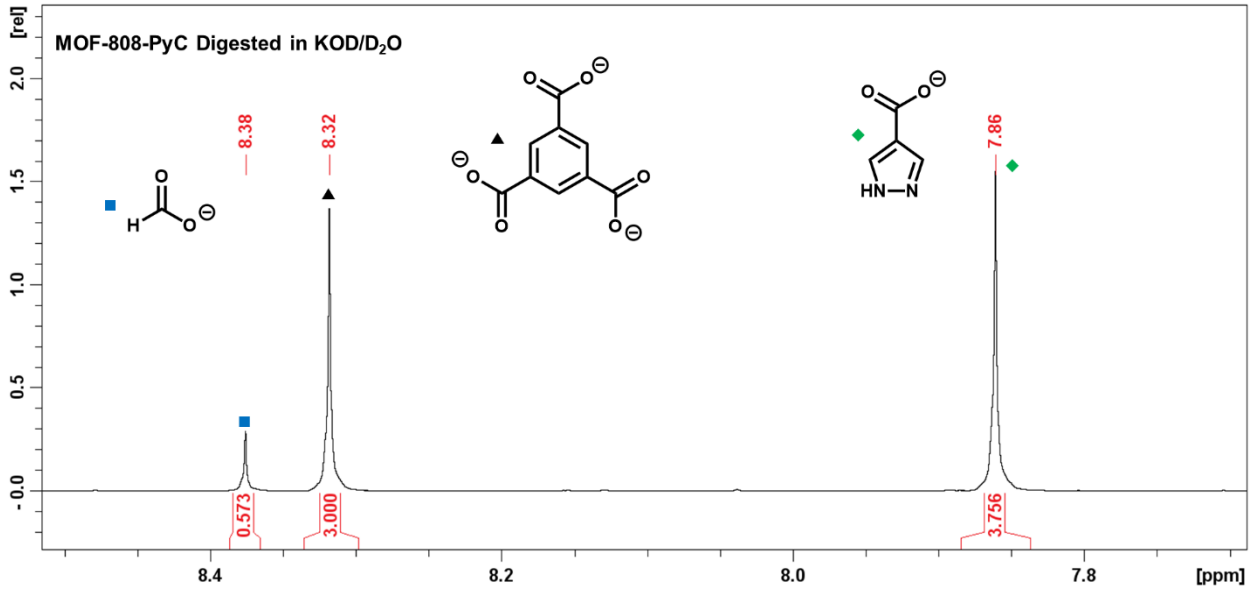

Figure S11. ^{1}H NMR spectrum of MOF-808-PyC digested in KOD/D_2O, zoomed in to show peaks used for quantification.

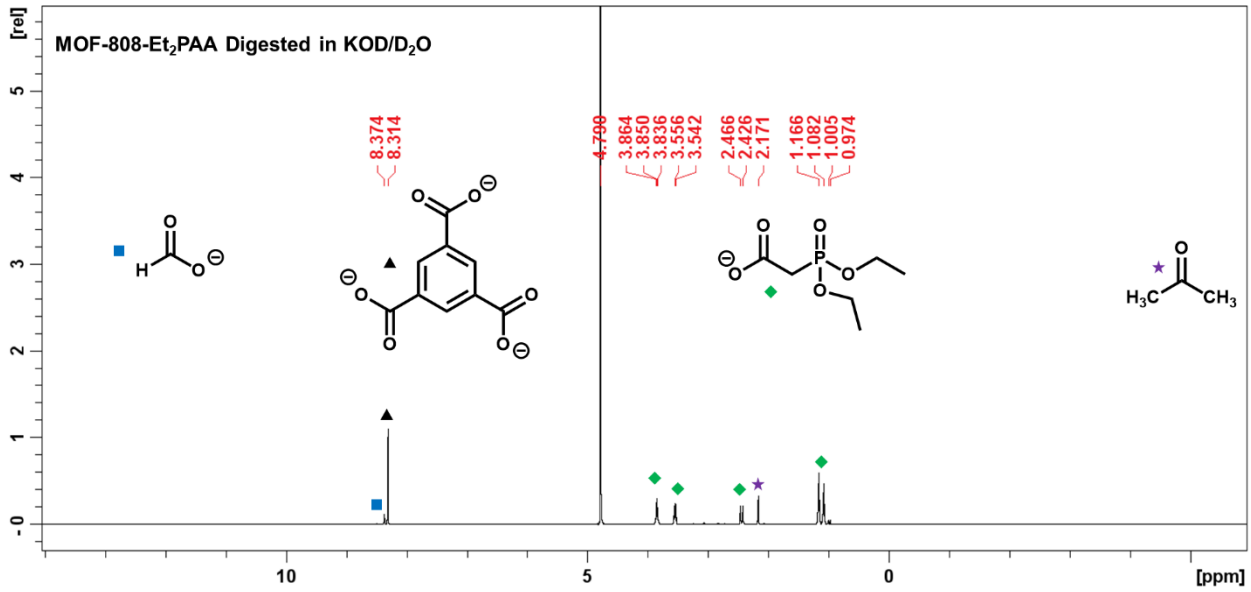

Figure S12. ^{1}H NMR spectrum of MOF-808-Et_2PAA digested in KOD/D_2O. Digestion resulted in partial hydrolysis of P-OEt groups. Green diamonds indicate all signals for Et_2PAA degradation products.

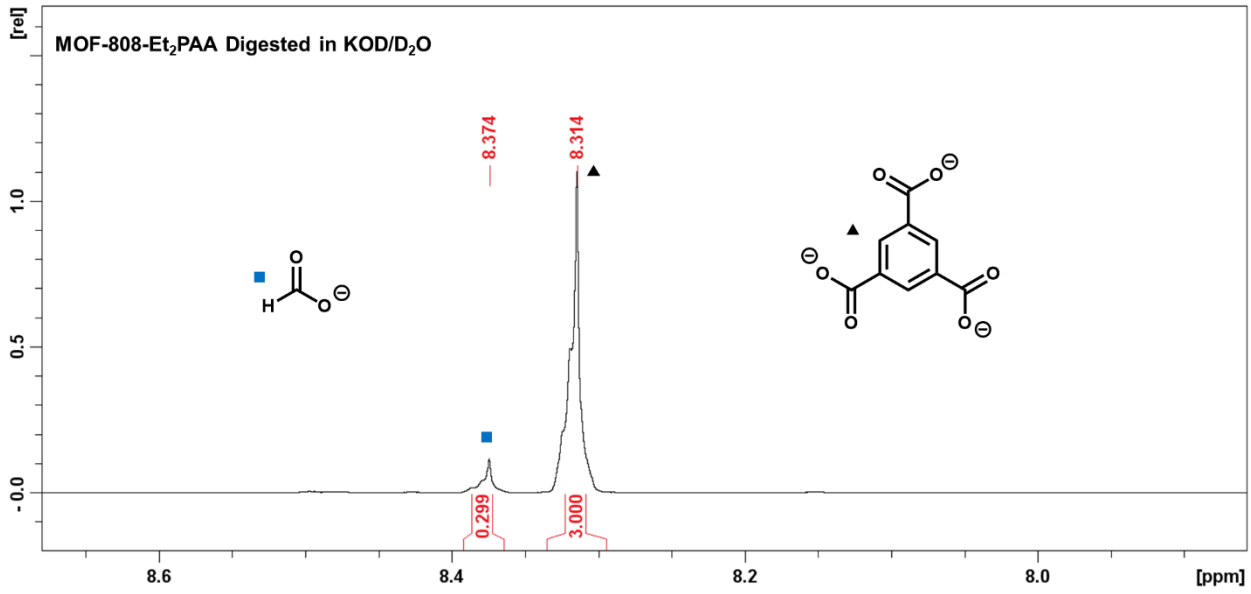

Figure S13. ^{1}H NMR spectrum of MOF-808-Et_2PAA digested in KOD/D_2O, zoomed in to show BTC and formate peaks used for quantification.

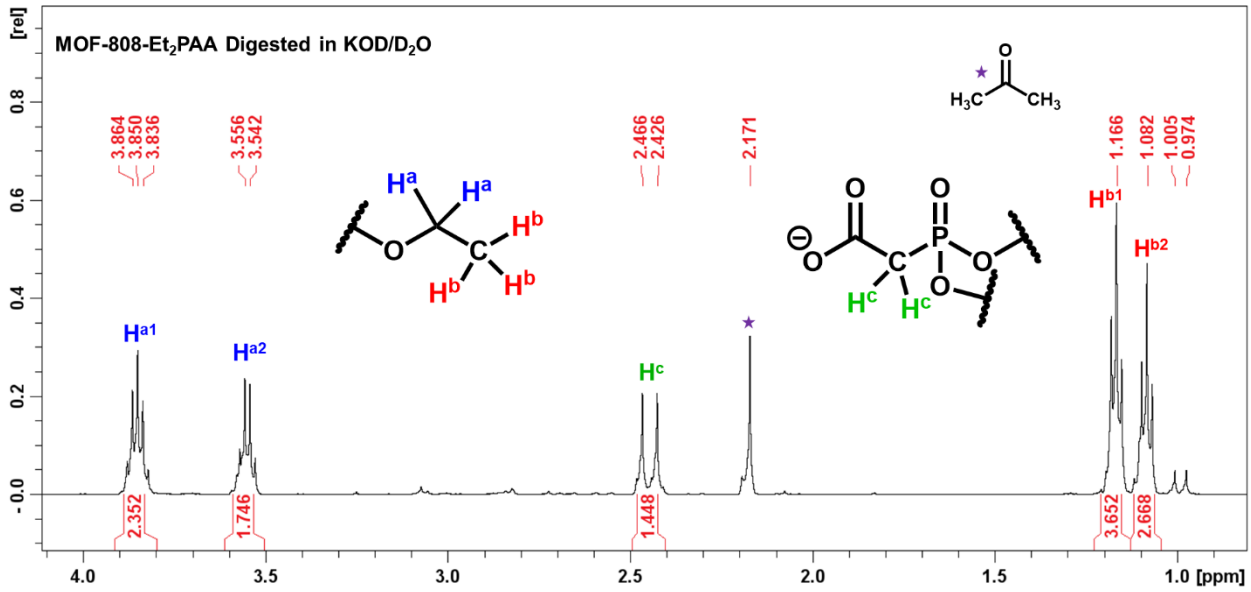

Figure S14. ^{1}H NMR spectrum of MOF-808-Et_2PAA digested in KOD/D_2O zoomed in to show peaks used for quantification. Digestion resulted in partial hydrolysis of P-OEt groups, giving multiple species, but protons corresponding to $-OCH_2CH_3$ groups were clearly identified (H^a and H^b). The identities of the degradation products were not determined unambiguously, but it was assumed that all $-OCH_2CH_3$ protons originated from Et_2PAA. As such, the integrations of H^{a1} and H^{a2} were added together, as were the integrations of H^{b1} and H^{b2}, to calculate the amount of Et_2PAA bound to the MOF prior to hydrolysis.

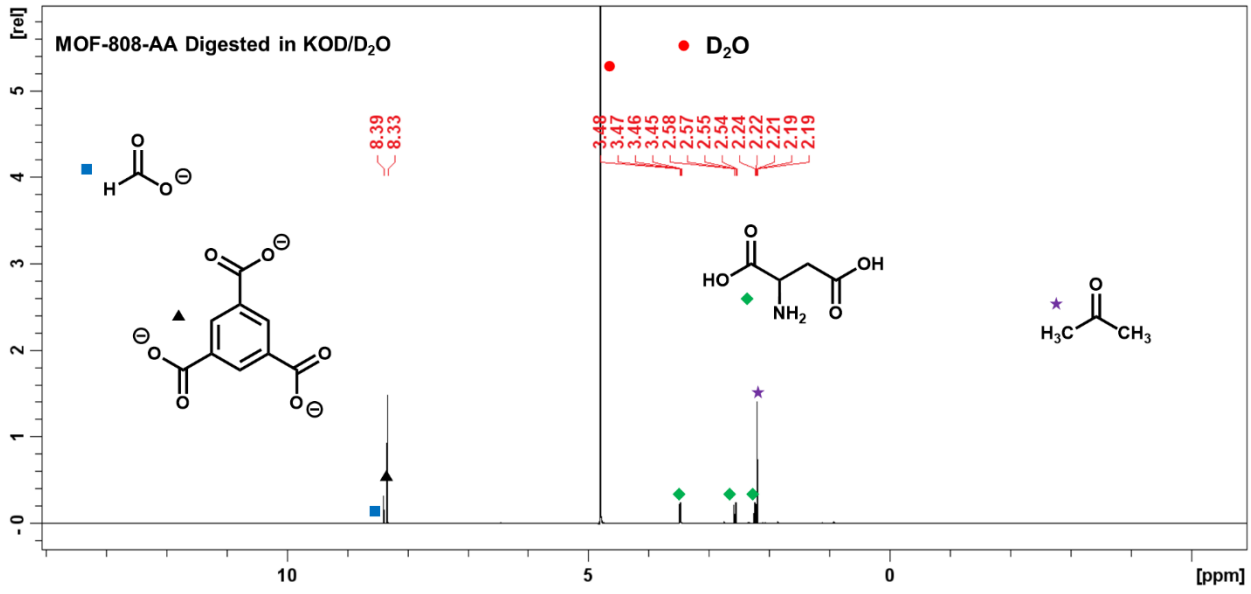

Figure S15. ^{1}H NMR spectrum of MOF-808-AA digested in KOD/D_2O. A small amount of acetone is present, likely due to incomplete activation.

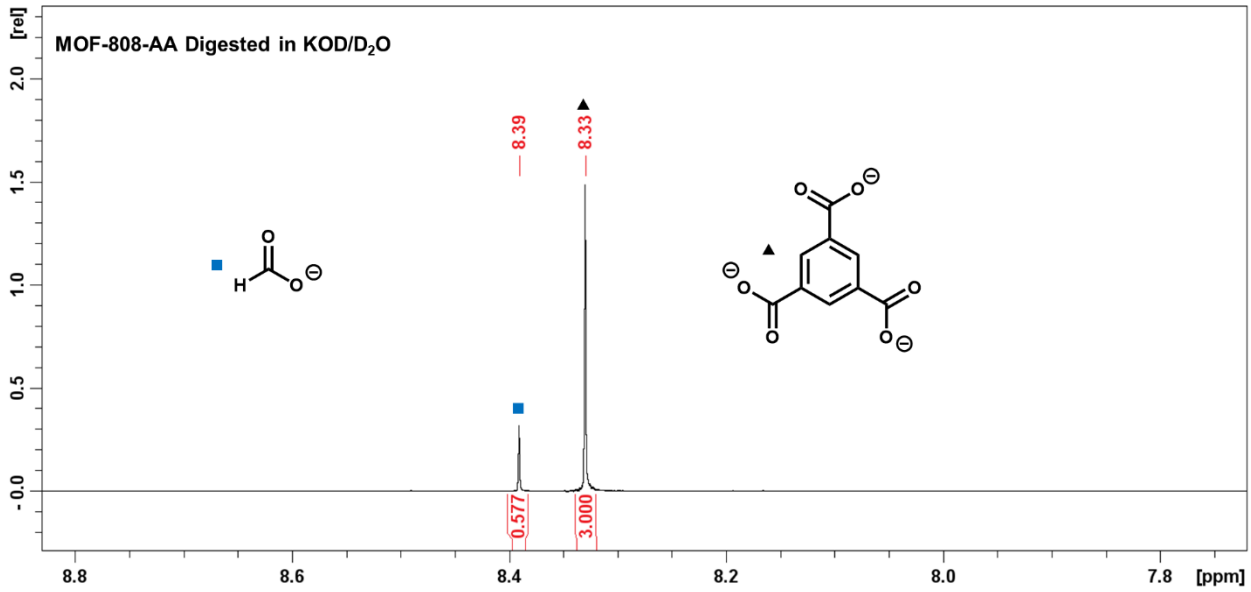

Figure S16. ^{1}H NMR spectrum of MOF-808-AA digested in KOD/D_2O, zoomed in to show BTC and formate peaks used for quantification.

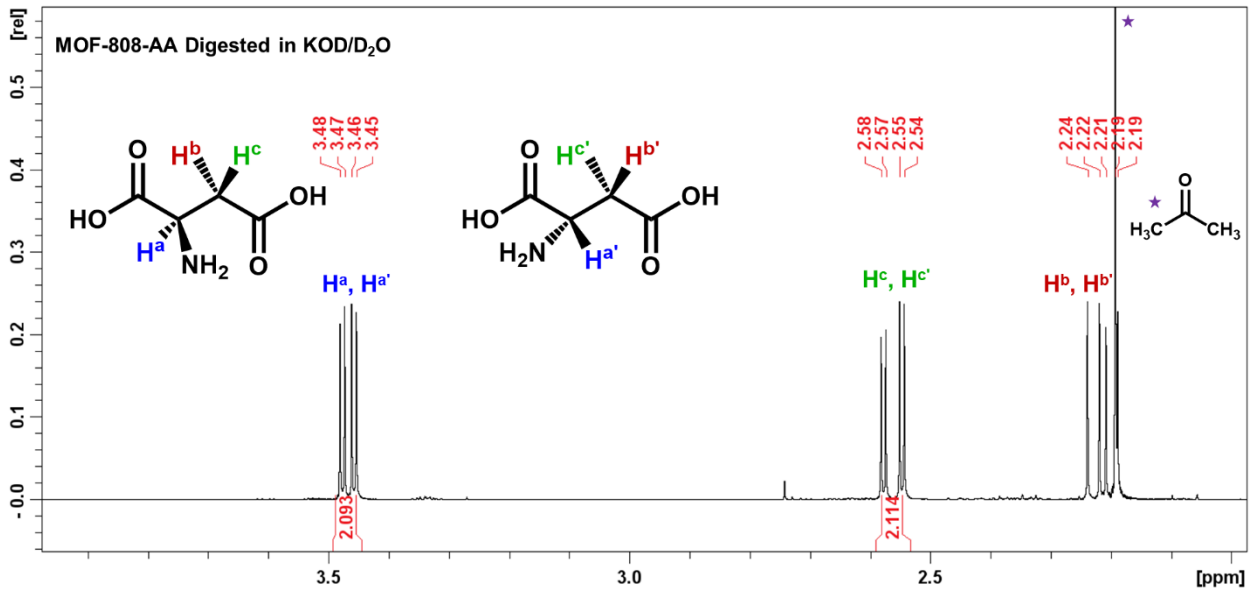

Figure S17. ^{1}H NMR spectrum of MOF-808-AA digested in KOD/D_2O, zoomed in to show aspartic acid peaks used for quantification. A minor acetone impurity overlaps with the peaks for H^{b} and $H^{b'}$.

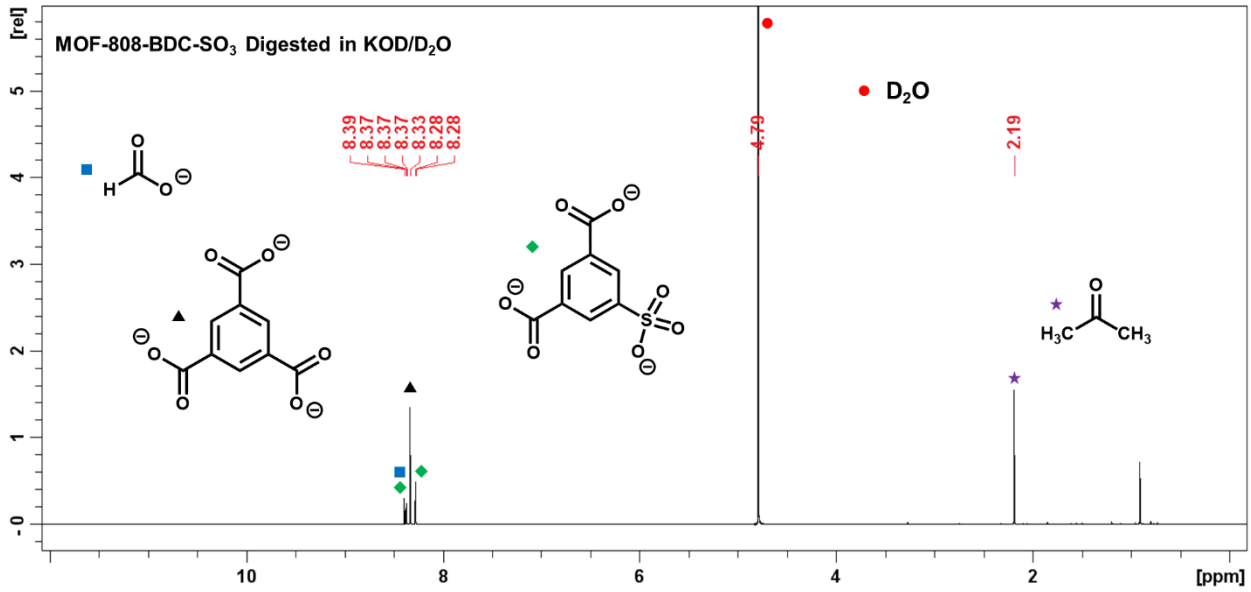

Figure S18. ^{1}H NMR spectrum of MOF-808-BDC-SO_3 digested in KOD/D_2O.

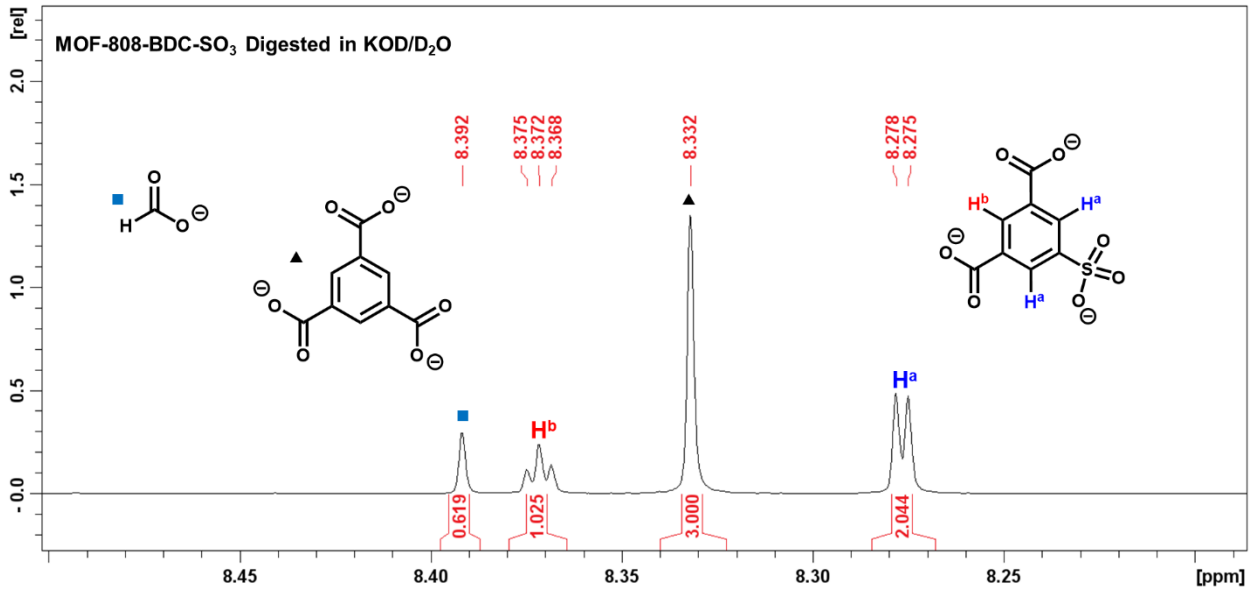

Figure S19. ^{1}H NMR spectrum of MOF-808-BDC-SO_3 digested in KOD/D_2O, zoomed in to show aromatic peaks used for quantification.

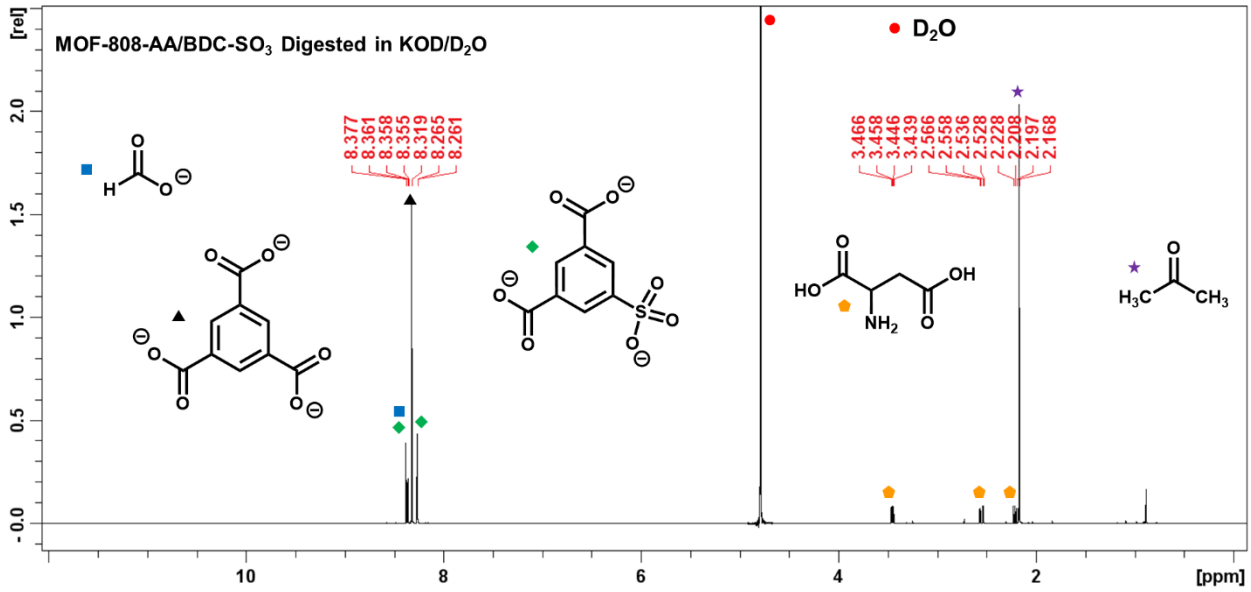

Figure S20. ^{1}H NMR spectrum of MOF-808-AA/BDC-SO_3 digested in KOD/D_2O.

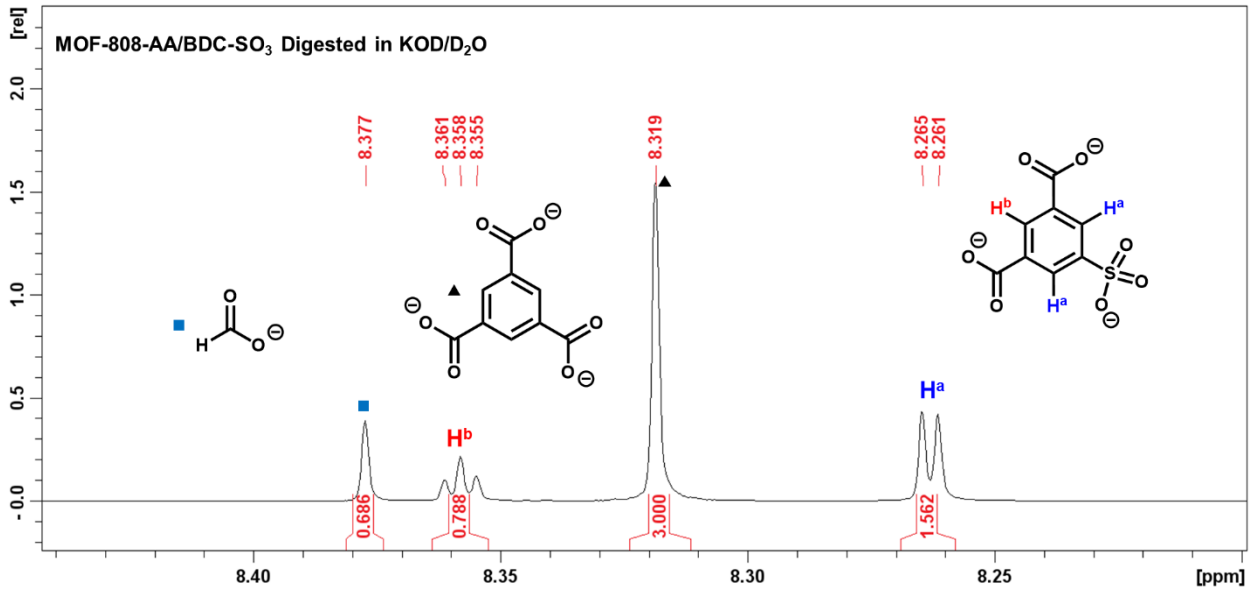

Figure S21. ^{1}H NMR spectrum of MOF-808-AA/BDC-SO_3 digested in KOD/D_2O, zoomed in to show aromatic peaks used for quantification.

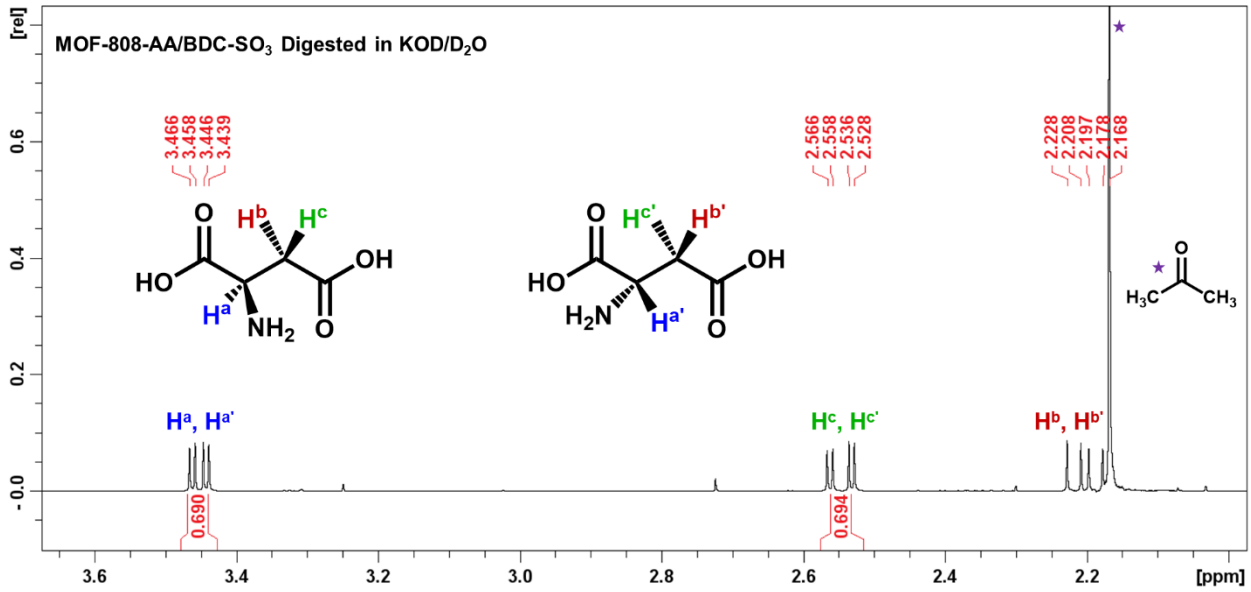

Figure S22. ^{1}H NMR spectrum of MOF-808-AA/BDC-SO_3 digested in KOD/D_2O, zoomed in to highlight AA peaks used for quantification.

Table S1. Number of functional groups per Zr_6 cluster in MOF-808 derivatives as determined by ^{1}H NMR of digested MOF samples.

MOF	# per cluster
MOF-808-PyC	3.7
MOF-808-Et_2PAA	2.1
MOF-808-AA	4.5
MOF-808-BDC-SO_3	2.1
MOF-808-AA/BDC-SO_3	1.4/1.6

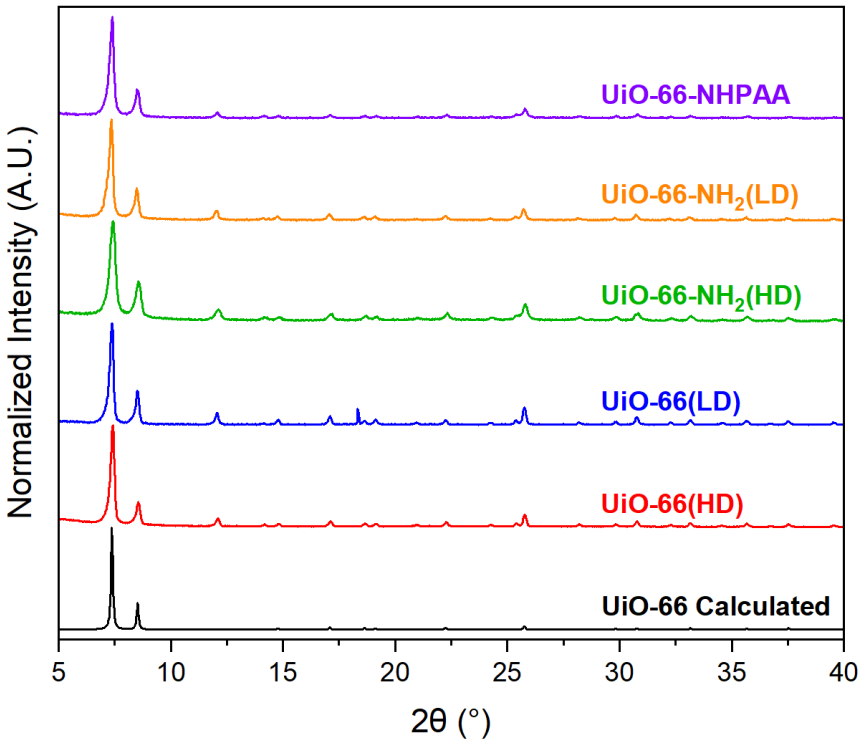

Figure S23. PXRD patterns of UiO-66 materials after competitive metal ion capture studies.

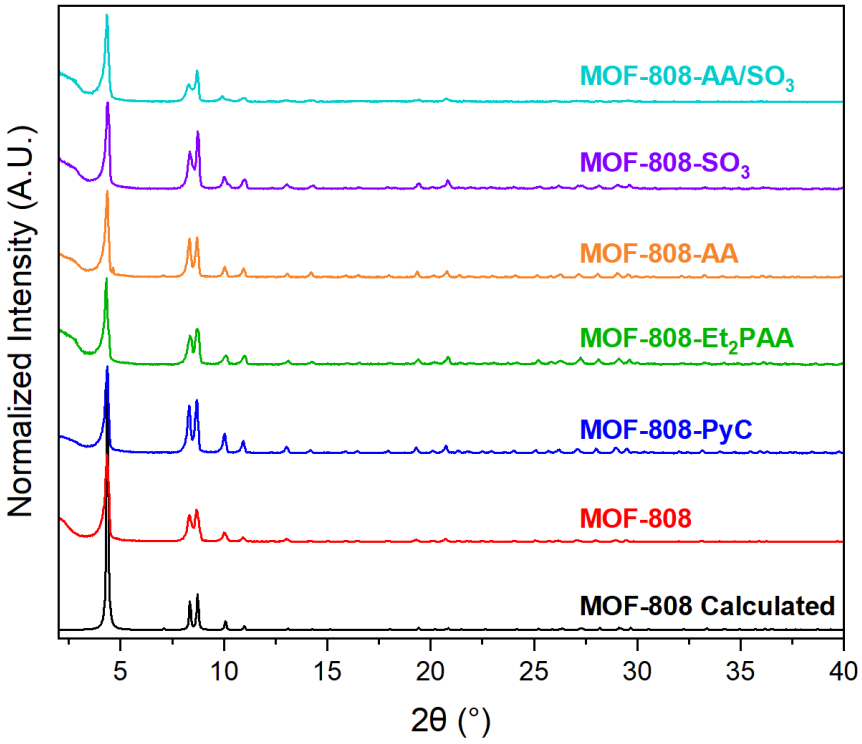

Figure S24. PXRD patterns of MOF-808 materials after competitive metal ion capture studies.

References

(1) Yuan, L.; Tian, M.; Lan, J.; Cao, X.; Wang, X.; Chai, Z.; Gibson, J. K.; Shi, W. Defect engineering in metal–organic frameworks: a new strategy to develop applicable actinide sorbents. *Chem. Commun.* **2018**, *54*, 370-373.

(2) Shearer, G. C.; Chavan, S.; Ethiraj, J.; Vitillo, J. G.; Svelle, S.; Olsbye, U.; Lamberti, C.; Bordiga, S.; Lillerud, K. P. Tuned to Perfection: Ironing Out the Defects in Metal–Organic Framework UiO-66. *Chem. Mater.* **2014**, *26*, 4068-4071.

(3) Peterson, G. W.; Destefano, M. R.; Garibay, S. J.; Ploskonka, A.; McEntee, M.; Hall, M.; Karwacki, C. J.; Hupp, J. T.; Farha, O. K. Optimizing Toxic Chemical Removal through Defect-Induced UiO-66-NH2 Metal–Organic Framework. *Chem. Eur. J.* **2017**, *23*, 15913-15916.

(4) Jiang, J.; Gándara, F.; Zhang, Y.-B.; Na, K.; Yaghi, O. M.; Klemperer, W. G. Superacidity in Sulfated Metal–Organic Framework-808. *J. Am. Chem. Soc.* **2014**, *136*, 12844-12847.